

STUDY OF THE PHASE TRANSITION AND PHYSICAL PROPERTIES OF AIAs, ScAs AND $Al_xSc_{1-x}As$ COMPOUNDS BY THE FP-LMTO METHOD

F. Betaoui¹, H. Rekab-Djabri^{2,3*}, K. Baddari⁴, S. Daoud⁵

¹*Computer Science and Mathematics Laboratory, Physics Department, Faculty of Science and Applied Science, AMO University, 10000, Bouira, Algeria*

²*Laboratory of Micro and Nanophysics (LaMiN), National Polytechnic School Oran, ENPO-MA, BP 1523, El M'Naouer, 31000, Oran, Algeria*

³*Faculty of Nature and Life Sciences and Earth Sciences, AMO University, 10000, Bouira, Algeria*

⁴*Ministry of Higher Education and Scientific Research, Algeria.*

⁵*Laboratory of Materials and Electronic Systems, Faculty of Sciences and Technology, University Mohamed El Bachir El Ibrahimi of Bordj Bou Arreridj, 34000 Bordj Bou Arreridj, Algeria*

**Corresponding author E-mail: h.rekabdjabri@univ-bouira.dz*

Article Info	Abstract
<p><i>Received: 28.01.2024</i> <i>Accepted: 20.03.2024</i></p> <p>Keywords: DFT, FP-LMTO, $Al_xSc_{1-x}As$ alloys, Structural properties, Electronic properties, thermal properties, optical properties.</p>	<p>In this present work, we will study the physical properties of a brand new semiconductor material. the structural stability and the electronic properties of Scandium Arsenide (ScAs) and Aluminum Arsenide (AIAs) semiconductors as well as their ternary alloys ($Al_xSc_{1-x}As$, $0 \leq x \leq 1$) in both rocksalt RS (B1) and zincblende ZB (B3). Calculations on both structures are done the method (FP-LMTO, <i>Full Potential Linear Muffin Tin</i>). In the framework of density functional theory (DFT). The exchange-correlation potential was calculated using both the <i>Local Density Approximation</i> and the <i>Generalized Gradient Approximation</i>.</p> <p>The structural parameters of $Al_xSc_{1-x}As$ alloys, such as the lattice constant, the bulk module and its derivative are calculated. The lattice parameter deviates slightly from the line of <i>Vegard's Law</i> in B3 structure, while the deviation was more pronounced in B1 structure.</p> <p>The calculations showed a phase transition from the ZnS phase (B3) to the RS phase (B1) at pressures (7, 10.5, 14.0 and 23.0 Gpa in LDA and (10.0, 12.5, 10.0 and 25.0 GPa) in GGA for $x = 0.25, 0.50, 0.75$ and 1.00) respectively. The calculated electronic properties showed that in phase B1, there exists an energy band (X-X) with a direct gap at $x = 0.00$. On the other hand, in phase B3, there are two kinds of energy bands, of direct gap ($\Gamma-\Gamma$) for $x = 0.25, 0.75$ and 1.00, the second band is of indirect gap ($\Gamma-X$) for $x = 0.50$, suggesting the possibility to be used in the long wavelength optoelectronic applications. The deviation of The calculated band gap deviation from linear behavior was significant in both structures. The $Al_xSc_{1-x}As$ alloys were found to be semiconducting at $x=0$ in the B1 phase and at $x=0.25, 0.50, 0.75$ and 1 in the B3 phase. Concerning calculations of the optical properties of the ternary $Al_xSc_{1-x}As$ alloy at concentrations $x= 0.25, 0.50$ and 0.75 in the ZnS (B3) phase, and from our bibliographic research we are sure that no reference exists in the literature. Our work can therefore be used as a reference for future research. Our simulation results are in good agreement with those obtained theoretically and experimentally.</p>

1. Introduction

The properties stability of the III-V semiconducting compounds are very important in many applications such as laser diodes, transistors and optic fibers in telecommunication. Their alloys are promising candidates for many device applications such as high-speed electronic and long wavelength photonic devices since their band gaps cover a wide spectral range. Aluminum Arsenide (AlAs) and Scandium Arsenide (ScAs) are binary compounds that have an experimental band-gap of about 2.16 eV [1], and 1.41 eV [2], respectively. The most stable phases for AlAs and ScAs are cubic zincblende (B3) and cubic rocksalt (NaCl-type or B1) respectively [1, 2]. Many searches by *A. Tebboune et al* [3] in NaCl(B1), CsCl(B2), ZnS(B3), Wurtzite (B4) and NiAs(B8) phases. A major advance according to *Y. Junhui et al* [4] on the ScAs semiconductor is that it is a ferroelastic material, and this behavior points it in the direction of applications for non-volatile memory devices. As well as their alloy ternaire $Al_xSc_{1-x}As$ in both cubic phases NaCl (B1) and ZnS (B3), including transitions of phases for three materials. Method FP-LMTO is introduced as part of the functional theory of density DFT, using the approximation of the generalized gradient GGA and the approximation of the local density LDA. These two theatrical approaches provided the solution that allowed the first basic quantum methods to develop and calculate total energy, energy band structure and DOS state density as well as all possible physical properties with very satisfactory accuracy. The *Lmtart Mindlab* calculation code in which the LMTO-PLW method is implemented is used.

Since the ternary compound AlScAs is a new material, little scientific research is available on its study. Therefore, the study of the physical properties of this compound is our goal of this project to improve these properties Then any further study will be novelty and out of our results. Before analyzing our results on the ternary compound (Arsenic of Aluminium and Scandium) $Al_xSc_{1-x}As$. I would like to say that during my bibliographic research I found only one reference by *W. Lopez-perez et al* [5], which studied its structural and electronic properties. Moreover, the comparison of the results will be based on this reference. The alloy $Al_xSc_{1-x}As$ is a benefit coming from the system AlAs/ScAs, both materials crystallize in stages ZnS (B3) and NaCl (B1) respectively. For this reason, in the course of our study, there may be a transition from the phase ZnS (B3) to the phase B1 of this alloy. According to the results, the NaCl (B1) phase of $Al_xSc_{1-x}As$ alloys is metallic while, but in the ZnS (B3) phase is a semiconductor. Their results showed also that the band gap undergoes a direct ($X \rightarrow X$) for $x=0.00$ in NaCl (B1) phase and for $x=0.25, 0.75, 1.00$ in B3 phase, to indirect ($\Gamma \rightarrow X$) transition for $x=0.50$ in ZnS (B3) phase at a given Al composition. The compositional dependence on the electronic properties of ternary alloy is suitable for the design and fabrication of high frequency

and high power electronic and optoelectronic devices. It is also used in laser diodes, as it has a narrow and direct gap.

The rest of this paper is organized as follows: a brief description of the method used is given in section two. The results and its discussion related to structural and electronic properties are presented in section three. Finally, conclusions are reported in section four.

2. Method of calculation

In this study, the calculations of the first principles were carried out using the linear muffin-tin orbital method with full FP-LMTO [6, 7] based on functional density theory, Calculated by the Mindlab software implemented in the Lmtart code. The structure of the energy band and the density of the electronic states of the chosen materials have been determined digitally and they are calculated in the manner of [8]. Furthermore, to deal with the correlation exchange, both approaches LDA and GGA were used, these two approximations are edited by *Perdew-Wang* 1991 [9]. FP-LMTO is an improved method over previous methods LMTO and is currently one of the most accurate calculation methods. The physical properties of solids. The basic functions are represented by Fourier series in the IR regions, while in the MT, the basic functions are represented in terms of the numerical solutions of the Schrödinger. Basic group LMTO and the charge density is augmented in harmonic spherical to $L_{max} = 6$. The use of the point k in the Brillouin zone corresponds to a grid of $2 \times 2 \times 2$, this alloy was also modeled using a super lattice of 64 atoms which corresponds to a cubic lattice. In order not to have an overlap of atoms for each atomic position, in each case the Mutin-Tin ray is different. To be clearer, total energy was an indispensable parameter to determine any physical property of any solid material. And to obtain this remarkable parameter it is necessary to go through the charge density. In certain materials, the instability of the structure leads to redistributions of the charge density to form a periodic spatial modulation. The latter is called charge density wave, an expression first discussed by *Fröhlich* [10, 11]. The modulation of the electron density modifies the ion potential in the network so that the ions move to new equilibrium positions, which explains the phase transition. Therefore, the charge density wave is always accompanied by a periodic grating distortion [12].

3. Structural properties

The structural parameters: the equilibrium lattice constant (a_{eq}), the compressibility module (B_{eq}) and its first derivative (B'_{eq}) were calculated for the ternary alloys $Al_xSc_{1-x}As$ according to the *Zunger* approach [13], which uses a super lattice of eight atoms. Before we

start it should be known that we are going to do the whole study of the physical properties in two cubic structures. That is to say, the elementary mesh of the crystal is defined three parameters a, b, c , where $a=b=c$ and $\alpha = \beta = \gamma = 90^\circ$, $a/b=1$ and $a/c=1$. Then alloys' unit cells were obtained from RS (B1) and ZB (B3) structures by replacing one, two, three and four As atoms by Al atoms, for the compositions $x=0, 0.75, 0.50, 0.25$ and 1, respectively. The resulting RS (B1) and ZB (B3) structures for binary compound have space group # 225, $Fm\bar{3}m$ and # 215, $P\bar{4}3m$ respectively at $x=0$ and $x=1$. The resulting B3 structure has space group # 215, $P\bar{4}3m$ for $x=0.25$ and $x=0.75$ while the composition of $x=0.50$ has space group # 16, $P222$. The atomic positions of binary and their ternary alloys in RS (B1) and ZB (B3) structures are shown in Fig. 1 and Table.1

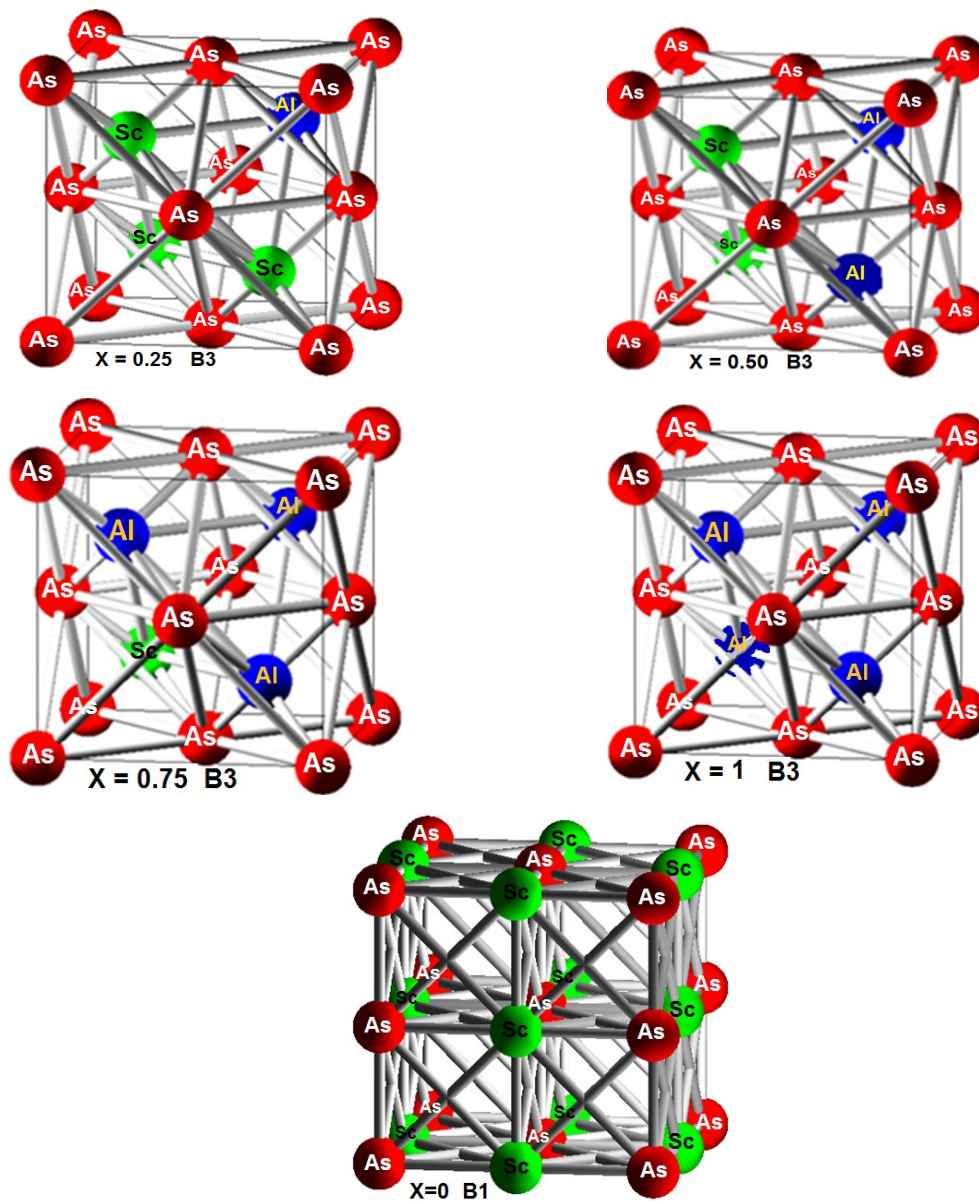


Figure 1. Cubic crystal structures of $Al_xSc_{1-x}As$ for composition x calculated by FP LMTO method

Table 1. Atomic positions for $Al_xSc_{1-x}As$ alloys.

Structure	x	Atom	Atomic position	
RokSalt (B1)	1.00	As	(0 0 0), (1/2 1/2 1/2), (1/2 1/2 0), (1.0 1.0 1/2)	
		Al	(1/2 0 1/2), (1.0 1/2 1.0), (0 1/2 1/2), (1/2 1.0 1.0)	
	0.75	As	(0 0 0), (1/2 1/2 1/2), (1/2 1/2 0), (1.0 1.0 1/2)	
		Sc	(1/2 0 1/2)	
		Al	(1.0 1/2 1.0), (0 1/2 1/2), (1/2 1.0 1.0)	
	0.50	As	(0 0 0), (1/2 1/2 1/2), (1/2 1/2 0), (1.0 1/2 1.0)	
		Sc	(1/2 0 1/2), (1.0 1/2 1.0)	
		Al	(0 1/2 1/2), (1/2 1.0 1.0)	
	0.25	As	(0 0 0), (1/2 1/2 1/2), (1/2 1/2 0), (1.0 1.0 1/2)	
		Sc	(1/2 0 1/2), (1.0 1/2 1.0), (0 1/2 1/2)	
		Al	(1/2 1.0 1.0)	
	0.00	As	(0 0 0), (1/2 1/2 1/2), (1/2 1/2 0), (1.0 1/2 1.0)	
		Sc	(1/2 0 1/2), (1.0 1/2 1.0), (0 1/2 1/2), (1/2 1.0 1.0)	
	Zinc Blende (B3)	1.00	As	(0 0 0), (1/2 0 1/2), (0 1/2 1/2), (1/2 1/2 0)
			Al	(1/4 1/4 1/4), (1/4 3/4 3/4), (3/4 3/4 1/4), (3/4 1/4 3/4)
0.75		As	(0 0 0), (1/2 0 1/2), (0 1/2 1/2), (1/2 1/2 0)	
		Sc	(1/4 1/4 1/4)	
		Al	(1/4 3/4 3/4), (3/4 3/4 1/4), (3/4 1/4 3/4)	
0.50		As	(0 0 0), (1/2 0 1/2), (0 1/2 1/2), (1/2 1/2 0)	
		Sc	(1/4 1/4 1/4), (1/4 3/4 3/4)	
		Al	(3/4 3/4 1/4), (3/4 1/4 3/4)	
0.25		As	(0 0 0), (1/2 0 1/2), (0 1/2 1/2), (1/2 1/2 0)	
		Sc	(1/4 1/4 1/4), (1/4 3/4 3/4), (3/4 3/4 1/4)	
		Al	(3/4 1/4 3/4)	
0.00		As	(0 0 0), (1/2 0 1/2), (0 1/2 1/2), (1/2 1/2 0)	
		Sc	(1/4 1/4 1/4), (1/4 3/4 3/4), (3/4 3/4 1/4), (3/4 1/4 3/4)	

Then, the unit meshes of the alloys were obtained from the structures B1 and B3 by replacing one, two, three and four atoms of As with atoms of Al, for the aluminum compositions $x = 0.00, 0.75, 0.50, 0.25$ and 1.00 respectively. Since our alloy crystallizes in the structure ZB (B3) for the aluminum compositions $x = 0.25, 0.50, 0.75$ and 1.00 , and in addition it crystallizes in the phase RS (B1) for the compositions $x = 0.00$. Then the structural parameters of the ground state were determined by calculating the total energy of the binary compounds and their alloys at different equilibrium volumes, in the structures RS (B1) and ZB

(B3). Then the calculated total energy values were adjusted to the *Murnaghan* state equation [14], (see Fig.2) which clearly shows that the energy differences calculated by the LDA approach are (-0.0080 eV) for $x = 0.00$ and (0.033, 0.038, 0.045 and 0.059 eV) for aluminum compositions $x = 0.25, 0.50, 0.75$ and 1.00 respectively.

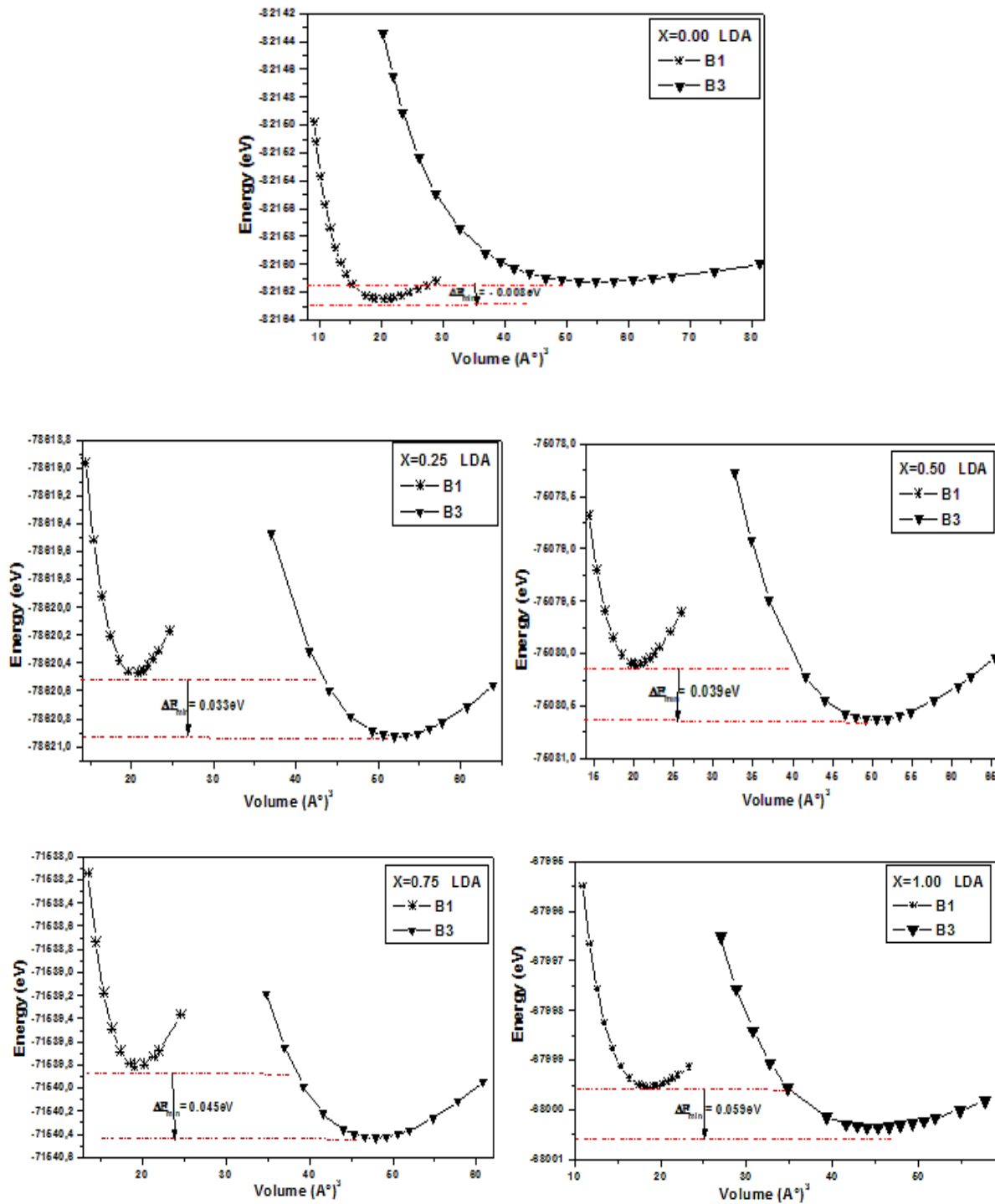


Figure 2. A). Variation of total energies as a function of the volume of the elementary mesh in phases RS (B1) and ZB (B3) of $\text{Al}_x\text{Sc}_{1-x}\text{As}$ ($x = 0.00, 0.25, 0.50, 0.75$ and 1.00) for LDA

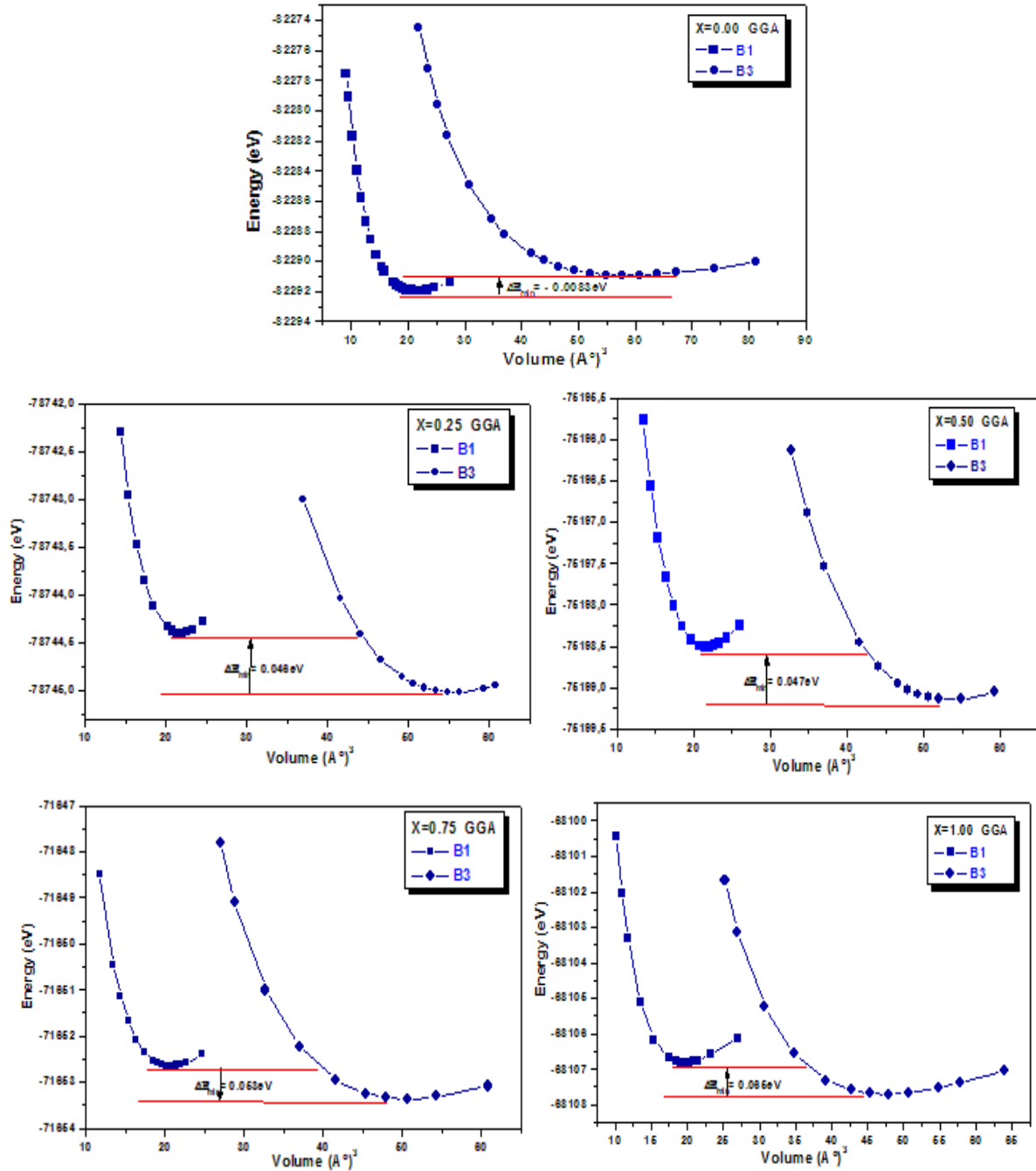


Figure 2.B) Variation of total energies as a function of the volume of the elementary mesh in phases RS (B1) and ZB (B3) of $Al_xSc_{1-x}As$ ($x = 0.00, 0.25, 0.50, 0.75$ and 1.00) for GGA

On the other hand, the approximation GGA underestimates the differences in energies with respect to the concentration $x=0.00$ is (-0.0083 eV) and (0.046, 0.047, 0.053, 0.065 eV) for $x=0.25, 0.50, 0.75$ and 1.00 respectively.

This means that the alloy is stable in the structure ZB (B3) for concentrations $x=0.25, 0.50, 0.75$ and 1.00 and still stable in the structure RS (B1) for $x=0.00$. The calculated structural parameters are listed in the (Table.2). In addition, compared with the experimental and theoretical results available with the two approximations LDA and GGA.

Our lattice constants calculated, for the structures *RS (B1)* and *ZB (B3)* of ScAs and AlAs, as indicated in the (Table.2), are in excellent agreement with the experimental results given in [15, 16], with a very small difference (approximately 0.02% for RS (B1) ScAs and 0.004% for B3 AlAs), and slightly better than other theoretical results [5, 17, 18]. The calculated values are underestimated in relation to the experimental values; this is a well-known trend in approximation LDA. The calculated values of the compressibility module are lower than the experimental values, due to the volume effect. The current results of the lattice constants for the *RS (B1)* and *ZB (B3)* structures of the ternary alloys $\text{Al}_x\text{Sc}_{1-x}\text{As}$ ($x = 0.25, 0.50, \text{ and } 0.75$) compare well with those measured experimentally for the compositions (0.00 and 1.00) [15, 16]. The lattice constant differs by $1.8 \cdot 10^{-4} \%$ and 0.001% from the experimental values measured at $x = 0.00$ and $x = 1.00$, respectively. To our knowledge, the B3 structure of $\text{Al}_x\text{Sc}_{1-x}\text{As}$ is very poorly synthesized and very few prior theoretical calculations exist for these alloys. Our data could be a prediction result for these ternary alloys in this structure. In (Fig.2), the difference in total equilibrium energies is plotted as a function of the concentration x of aluminum of the two phases *RS (B1)* and *ZB (B3)* and by the two approximations LDA and GGA.

Figure 3 shows that the transition occurs approximately around $x < 0.25$. In the case of $\text{Al}_x\text{Sc}_{1-x}\text{As}$, the transition *ZB (B3)* \rightarrow *RS (B1)* occurs approximately at $x = 0.15$ per LDA. Thus, it can be concluded that below this value, it is preferable to manufacture a system of AlAs/ $\text{Al}_x\text{Sc}_{1-x}\text{As}$ material because AlAs and $\text{Al}_x\text{Sc}_{1-x}\text{As}$ both crystallize in the structure *ZB (B3)*. However, for $x > 0.15$, it is preferable to manufacture a system of material ScAs/ $\text{Al}_x\text{Sc}_{1-x}\text{As}$ because both materials should crystallize in the structure B1 with a grating shift of only 0.037% for the system ScAs/ $\text{Al}_{0.50}\text{Sc}_{0.50}\text{As}$. As a result, a linear variation is observed and it can be reported that our alloy $\text{Al}_x\text{Sc}_{1-x}\text{As}$ crystallizes in the structure *RS (B1)* for compositions (x) below 0.15 and 0.25, per LDA and per GGA. In addition, the same alloy $\text{Al}_x\text{Sc}_{1-x}\text{As}$ crystallizes in the structure *ZB (B3)* for compositions (x) greater than 0.15 and 0.25 per LDA and per GGA. Unfortunately, as mentioned above, the lack of data for $\text{Al}_x\text{Sc}_{1-x}\text{As}$ in the literature did not allow us to have an approximation. Idea of the error in our transition value $x = 0.15$. However, it is assumed that the error may not be significant because convergence tests have shown that the compound ScAs and the associated ternaries $\text{Al}_x\text{Sc}_{1-x}\text{As}$ converge rapidly.

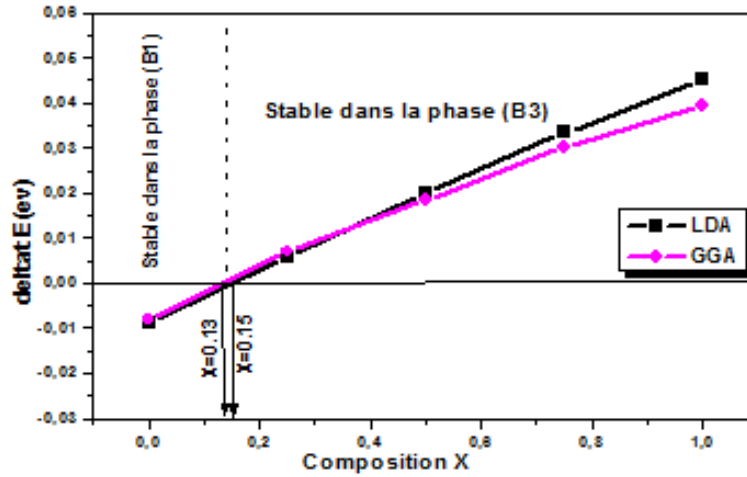


Figure 3. Variation of the most stable total energy difference of phases RS (B1) and ZB (B3) as a function of Al concentration, with LDA and GGA

Table 2. Calculated lattice parameter (a) and bulk modulus (B) compared to experimental and other theoretical values of ScAs and AlAs and their alloys $Al_xSc_{1-x}As$.

^ Ref. [9]* Ref. [19]** Ref. [20]*** Ref. [7]

	a (Å)		B (Gpa)				B'					
	This work		Expt	Other Calcul		This work		Other Calcul				
	LDA	GGA		LDA	GGA	LDA	GGA	LDA	GGA			
RS (B1)												
AlAs	5.305	5.401		5.210	5.303 [^]	82.969	78.114	91.430 [^]	80.823 [^]	3.659	3.426	
Al _{0.75} Sc _{0.25} As	5.382	5.491		5.257	5.363 [^]	80.615	69.729	89.938 [^]	78.620 [^]	3.549	3.599	
Al _{0.5} Sc _{0.5} As	5.461	5.580		5.294	5.409 [^]	74.584	67.228	92.949 [^]	79.765 [^]	3.689	3.409	
Al _{0.25} Sc _{0.75} As	5.466	5.596		5.33	5.460 [^]	76.790	67.375	93.436 [^]	80.189 [^]	3.719	3.528	
ScAs	5.463	5.594	5.464 [*]	5.472 ^{***}	5.491 [^]	101.798	85.911	102.975 ^{***}	83.475 [^]	3.075	3.087	2.945 ^{**}
ZB (B3)												
AlAs	5.655	5.764	5.661 ^{**}	5.631	5.730 [^]	71.494	63.550	74.844 [^]	66.483 [^]	3.618	3.492	
Al _{0.75} Sc _{0.25} As	5.764	5.881		5.743	5.854 [^]	65.463	61.344	68.883 [^]	60.942 [^]	3.829	3.231	
Al _{0.5} Sc _{0.5} As	5.869	5.977		5.839	5.961 [^]	62.816	62.962	65.324 [^]	57.930 [^]	3.329	2.905	
Al _{0.25} Sc _{0.75} As	5.942	6.063		5.917	6.047 [^]	61.638	59.284	63.480 [^]	56.623 [^]	3.231	2.896	
ScAs	6.034	6.174		5.977	6.117 [^]	62.521	54.724	62.733 [^]	54.425 [^]	3.603	2.756	3.408 ^{***}

4. Thermodynamic properties Phase transition

The lowest Gibbs free energy indicates the stability of a structure regardless of the data by $G = E + PV - TS$, where E is the internal energy, S represents the vibrational entropy, P is the given pressure and V represents the volume. Since the calculations have been carried out at $T = 0$ °K, the Gibbs equation G is then equivalent to enthalpy $H = E + PV$ and the pressure

P for which the Gibbs energies of the two phases are equal is defined as the transition between these two phases. Our calculations show that the configuration of the ground state is the NaCl type structure. It is possible to deduct from it a possibility of transition under pressure, of phase ZB (B3) towards stage B1. The enthalpy as a function of the pressure for the phase (Fig.4.a) is illustrated on LDA and (Fig.4.b) is illustrated on GGA $Al_xSc_{1-x}As$ for the alloy B1 with reference to the structure ZB (B3). The results obtained show that $Al_xSc_{1-x}As$ undergoes only one structural phase transition under pressure. The phase transition (ZB (B3) \rightarrow RS (B1)) should occur at (7.00. 10.50. 14.00. 23.00 Gpa) and (10.00. 12.50. 16.00. 25.00 Gpa) for composition X = 0.25. 0.50. 0.75. 1.00, using both approximations LDA and GGA, with a remarkable volume reduction for LDA and GGA, see (Table.2). At the best of our research, no theoretical or experimental results have been found to make a comparison therefore; our result will be a reference for future work.

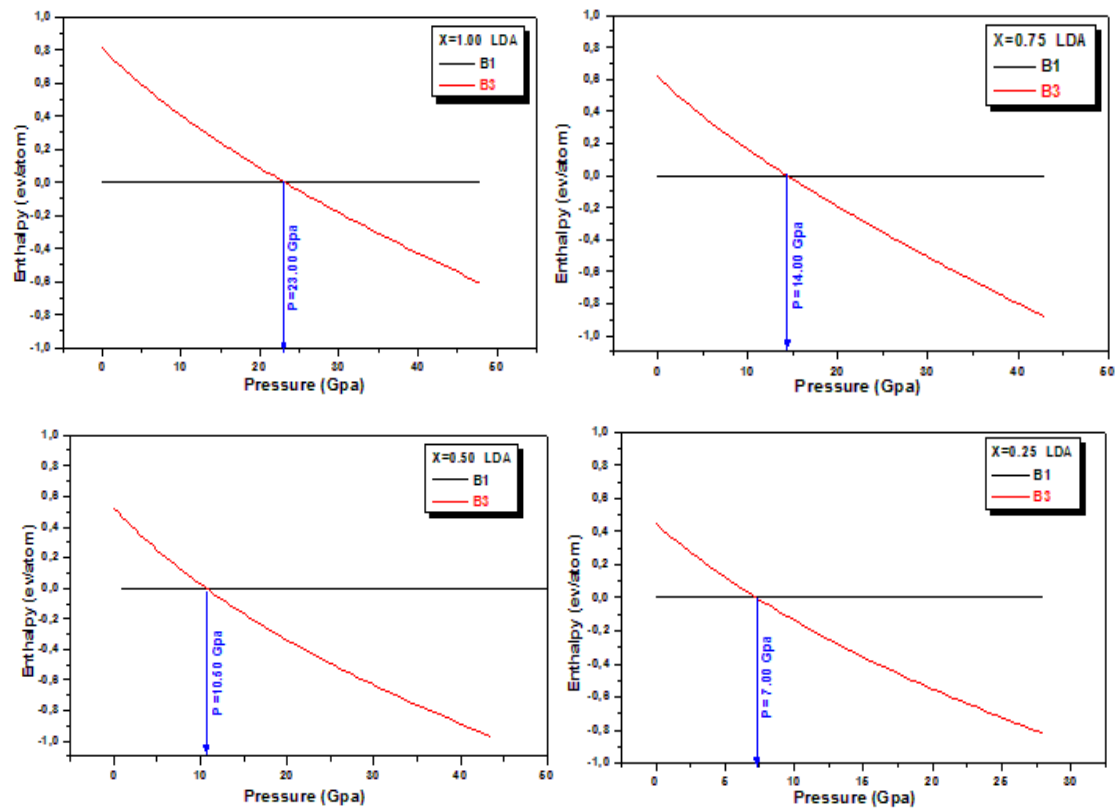


Figure 4. a) Variation of enthalpy differences ΔH as a function of pressure for phase RS (B1) and ZB (B3) of alloy $Al_xSc_{1-x}As$ for LDA.

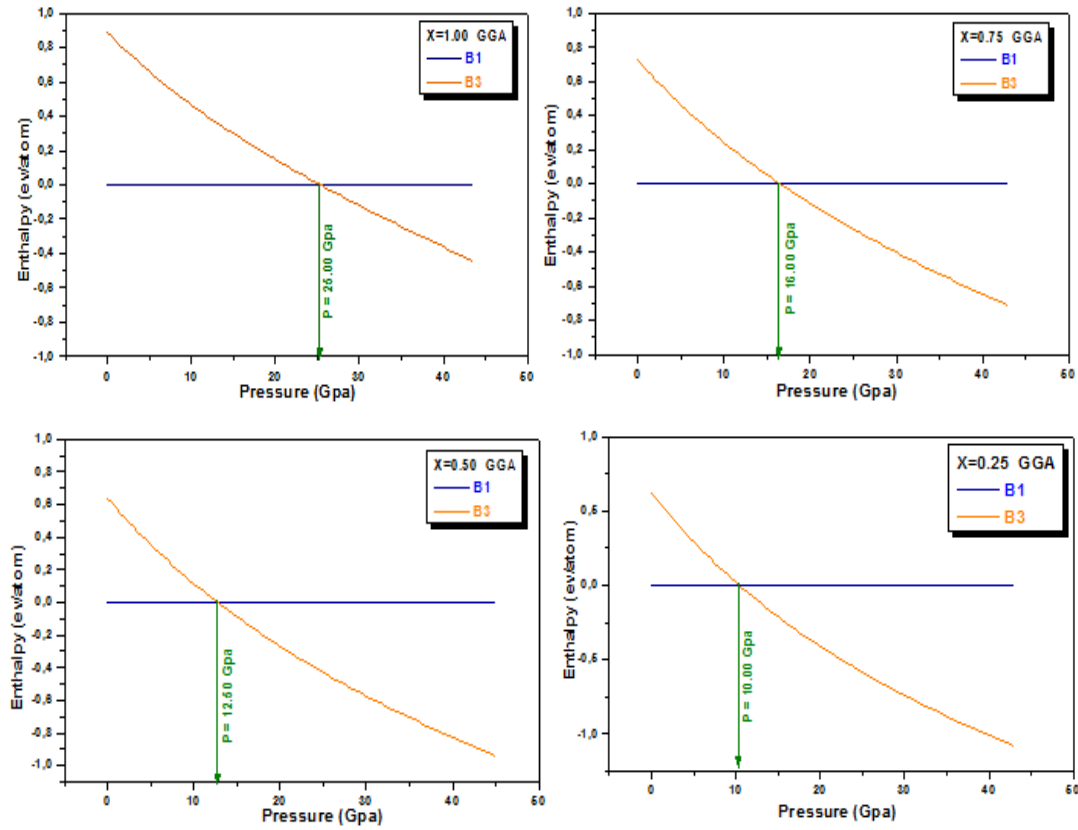


Figure 4. b) Variation of enthalpy differences ΔH as a function of pressure for phase RS (B1) and ZB (B3) of alloy $Al_xSc_{1-x}As$ for GGA.

Following the detailed explanation of the phase transition, Table.3 summarizes all the calculated values of the transition pressures (Gpa), the equilibrium volumes of the two phases *RS (B1) and ZB (B3)* and their differences in volt electron volumes. To add of course that the calculations were obtained by the two approaches LDA and GGA. This same table shows that as the concentration of aluminum x increases, the pressure increases, the volume and the difference in volume decreases. For that there was a phase transition following a volume compression.

Table.3. Evaluation of the transition pressures as a function of the concentration x of aluminum by the two approximations LDA and GGA.

x	P (Gpa)		V (eV) B1		V (eV) B3		ΔV (eV)	
	LDA	GGA	LDA	GGA	LDA	GGA	LDA	GGA
0.25	7,00	10,00	40,827	43,809	52,449	55,718	11,622	11,908
0.50	10,50	12,50	40,715	43,435	50,539	53,381	9,824	9,946
0.75	14,00	16,00	38,974	41,389	47,875	50,850	8,902	9,460
1.00	23,00	25,00	37,325	39,388	45,210	47,875	7,886	8,487

The grating constant decreases with the increase in the $Al(x)$ composition, as shown in (Fig.5). Indeed, the scandium atom is heavier than the aluminum atom because of their atomic masses. The same face shows that the constants of network calculated for different concentration of alloy in structure B3 obeys the law of *Vegard* with a light incline parameter. Downwards to $-0,064\text{\AA}$ and (-0.036\AA) respectively by LDA and GGA, this means that the deviation from Vegard's law is in very good agreement with those obtained by Ref [5] which were (-0.048\AA) with GGA and (-0.064\AA) with LDA. Furthermore, in phase B1, the inclination parameter is slightly pronounced by (-0.29\AA) with GGA and (-0.27\AA) with LDA. These inclination parameters were obtained by adjusting the calculated values of (a) with the following second-order polynomials.

$$a(x)^{B3\text{ GGA}} = 6.17 - 0.37x - 0,036x^2 \quad a(x)^{B3\text{ LDA}} = 6,03 - 0,31x - 0,064x^2 \quad (1)$$

$$a(x)^{B1\text{ GGA}} = 5.59 + 0.19x - 0,29x^2 \quad a(x)^{B1\text{ LDA}} = 5.46 - 0,11x - 0,27x^2 \quad (2)$$

This difference is mainly due to the concordance of the lattice constants of the alloy $Al_xSc_{1-x}As$ is 0.03% for $(x = 0.00)$ in structure B1 and 0.07% for structure B3. Compared to *Vegard's* prediction (black dotted line) and the theoretical line Ref [5].

Furthermore, the bulk modulus as a function of the composition x increases with the increase in the concentration of $Al(x)$, as shown in (Fig.6), which indicates that when x increases from $x = 0.00$ to $x = 1.00$, the alloys become less compressible and we can see the linearity from $x = 0.75$ to $x = 1.00$.

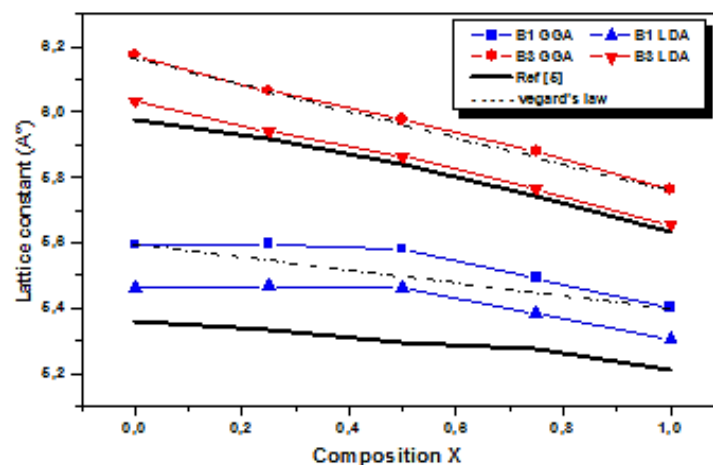


Figure 5. Presentation of the network constant as a function of the aluminum concentration x of the $Al_xSc_{1-x}As$ in phases RS (B1) and ZB (B3) by LDA and GGA

The bulk module has been adjusted with the following polynomials of the second order:

$$B(x)^{B3\ GGA} = 55.17 + 14.75x - 6.86x^2 \quad (3)$$

$$B(x)^{B3\ LDA} = 62.62 - 8.77x + 17.48x^2 \quad (4)$$

There is a significant deviation from linear concentration dependence with an upward inclination parameter of (-6.86 Gpa) for (GGA) and down (17.48 Gpa) for (LDA) in the ZB (B3) structure, by a difference of 0.2% for (LDA) and 1.7% for (GGA) in comparison with the result found by *W. López-pérez et al* [5].

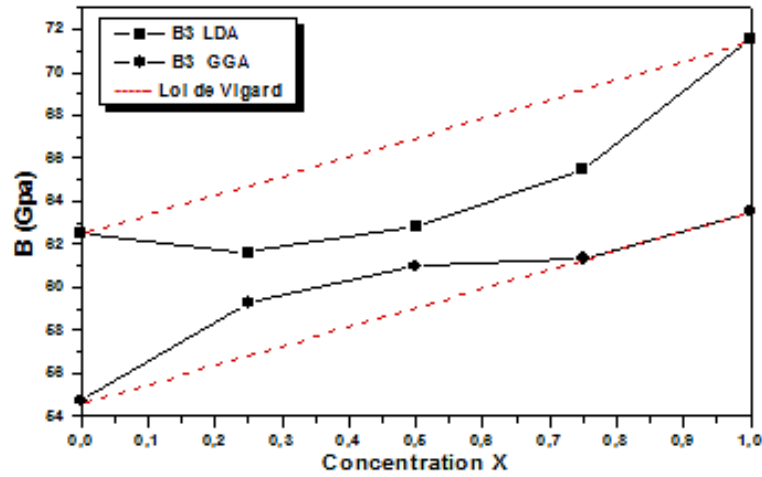


Figure 6. Dependence on compressibility modulus composition calculated in structures RS (B1) and ZB (B3) of $Al_xSc_{1-x}As$ alloy compared with linear concentration dependence prediction, by LDA and GGA

5. Electronic properties

5.1. Band structure

The strip structure of semiconductor materials plays an important role in the manufacture of electronic and optoelectronic devices. Based on the optimized structural results, the electronic band structures to the calculated lattice constants were obtained by the approximations LDA and GGA in the structures *RS (B1) and ZB (B3)*. The (*Fig. 7*) shows, as a prototype, the band structure of the alloy $Al_xSc_{1-x}As$ at $x = 0.00$ in the structure B1 and at $x = 0.50$, $x = 1.00$ in ZB (B3) structures. The Fermi level (E_F) coincides with the top of the valence band, as shown in (*Fig. 7*).

It may be noted that for composition $x = 0.00$ the minimum of the conduction band is greater than the maximum of the conduction band at point X of B1, And for compositions

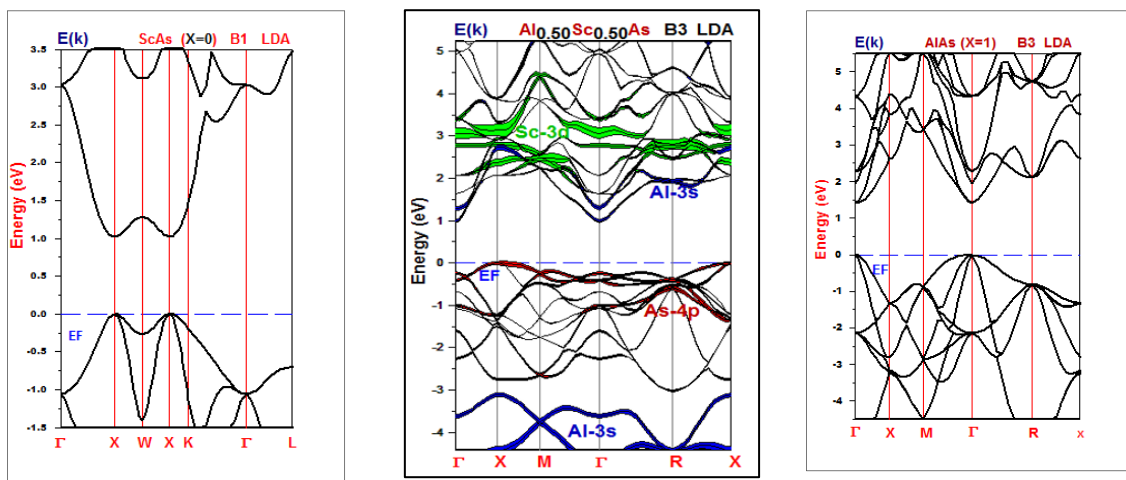
$x=1.00$, 0.25 and 0.75 the minimum of the conduction band is greater than the maximum conduction band at point Γ , this means that the four compositions are direct forbidden band compounds in the structure RS (B1) for $x = 0.00$ and in the structure B3 for $x = 1.00$, 0.25 and 0.75. On the other hand, at $x = 0.50$, the conduction band has a minimum at point Γ and the conduction band has a maximum at point X in the structure B3, indicating that in the structure B3 the ternary compound has indirect forbidden bands.

Calculated values of the forbidden energy band for each composition studied ($x = 0.00$, 0.25, 0.50, 0.75 and 1.00) in structures RS (B1) and ZB (B3) are given in (Table.4), compared with other available theoretical data. Again, the values listed clearly show that the calculated energy band has direct forbidden bands (Γ - Γ) and (X - X) for the binary compounds AlAs and ScAs RS (B1) and ZB (B3), their ternary alloys $Al_xSc_{1-x}As$ in phase B3 have direct forbidden bands (Γ - Γ) for $Al_xSc_{1-x}As$ ($0 \leq x \leq 1$), except in $x = 0.50$ have an indirect forbidden band (X - Γ) in ZB (B3).

Table 4. Evaluation of direct and indirect forbidden bands calculated in structures RS (B1) and ZB (B3) of alloys $Al_xSc_{1-x}As$ ($x = 0.00, 0.25, 0.50, 0.75$ and 1.00)

	$\Gamma \rightarrow X$				exp	$\Gamma \rightarrow \Gamma$				$X \rightarrow X$			
	This Work		Other Works			This Work		Other Works		This Work		Other Works	
	LDA	GGA	LDA	GGA		LDA	GGA	LDA	GGA	LDA	GGA	LDA	GGA
0.00	1.416	1.342	1.903	1.981*	2.240 [^]	3.036	3.075	3.229	3.323*	1.981	2.194	1.342	1.435*
0.25	0.861	1.057	2.098	2.145*		1.816	1.966	2.112	2.137*	1.803	1.978	1.615	1.676*
0.50	0.515	0.821	2.050	2.106*		2.066	2.159	1.514	1.469*	1.647	1.797	2.059	2.104*
0.75	0.377	0.633	1.762	1.864*		1.602	1.658	1.434	1.318*	1.515	1.652	2.675	2.721*
1.00	0.448	0.494	1.232	1.420*		1.401	1.542	1.872	1.685*	1.45	1.543	3.463	3.526*

[^]Ref. [21]* Ref. [25]



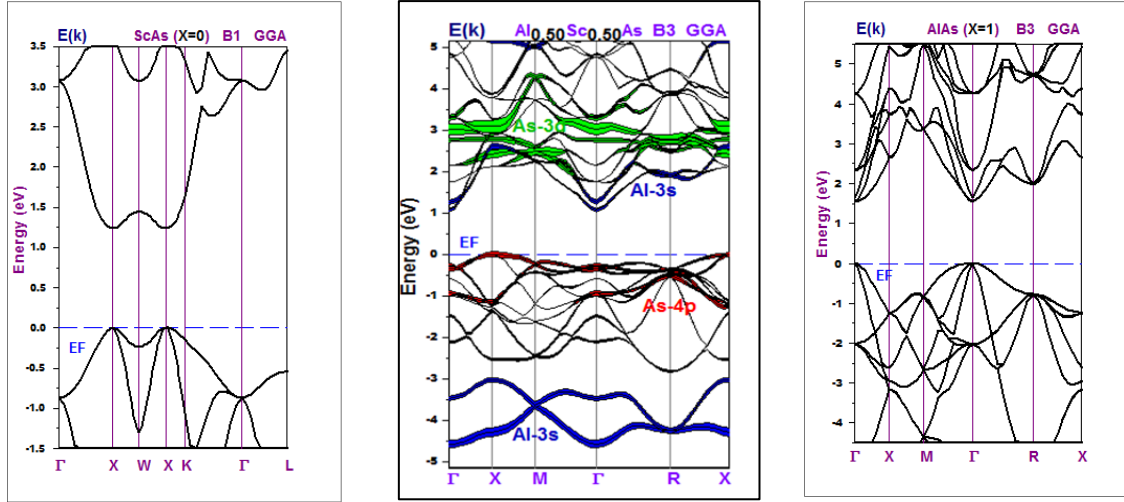


Figure 7. Presentation of the band structure of the alloy $\text{Al}_x\text{Sc}_{1-x}\text{As}$ ($x=0.00$, $x=0.50$ and $x=1.00$) in phases RS (B1) and ZB (B3) calculated by LDA and GGA

In fact, it is well known that LDA underestimates experimental value strongly, that the structure of got band has the good order of levels of energy and in form of bands in comparison with experimental value, because LDA does not take into account the self-examination of almost particles. The energy is taken into account and therefore the correlation exchange and its charge derivative cannot be reproduced correctly. Moreover, the values calculated in the DFT are at $T = 0^\circ\text{K}$, whereas the experimental values are generally measured at ambient temperature. This means that the contribution of the lattice vibrations is not taken into account in the present calculations. Although the lattice constant may follow *Vegard's law*, this is not the case with the banned band. It deviates from the linear mean and can be expressed as follows:

$$E_g(x) = xE_g^{\text{AlAs}} + (1-x)E_g^{\text{ScAs}} - x(1-x)b \quad (5)$$

where E_g^{AlAs} and E_g^{ScAs} are respectively the energy differences of the binary compounds AlAs and ScAs. The (Fig.8) shows the forbidden band energies $E_g(x)$ calculated as a function of the aluminum concentration. In the structure RS (B1), it is clear that E_g decreases nonlinearly with the increase in the aluminum concentration until $x=1.00$. In structure ZB (B3), the energy of the prohibited band, as stated in The same face diminishes linearly with the increase of aluminum concentration. The deviation from *Vegard's Law* is more pronounced in phase ZB (B3) than in phase RS (B1). The total inclination parameter was calculated by adjusting the nonlinear variation of the forbidden bands calculated as a function of concentration (x) with a quadratic function, as in the following equations:

$$E_g(\Gamma-X)^{B1\text{ LDA}}(x) = 1.416 - 2.636x + 1.668x^2 \quad (6.a)$$

$$E_g(\Gamma-X)^{B1\text{ GGA}}(x) = 1.342 - 1.236x + 0.388x^2 \quad (6.b)$$

$$E_g(X-X)^{B3\text{ LDA}}(x) = 1.981 - 0.759x + 0.183x^2 \quad (7.a)$$

$$E_g(X-X)^{B3\text{ GGA}}(x) = 2.194 - 0.937x + 0.286x^2 \quad (7.b)$$

As can be seen, from the equations. (6.a, 6.b) and (7.a, 7.b), the tilt parameters for the structure RS (B1) in the approximations LDA and GGA are (1.668eV, 0.388eV) and are greater than the tilt parameter for the structure ZB (B3) in approximation LDA and GGA (0.183eV, 0.286eV), which is consistent with it is thought that the deviation of the energies of the forbidden band is the result of the lattice constant and of the electronegativity shift of the parent atoms.

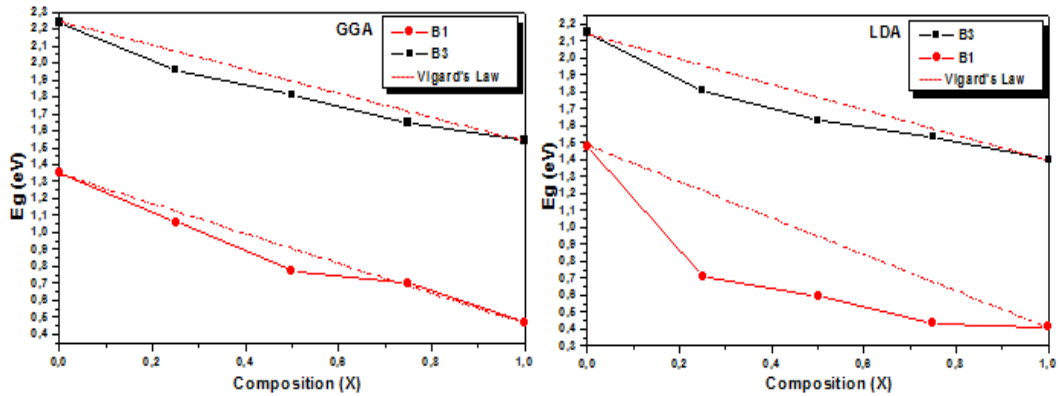


Figure 8. Graphical presentation of the energy dependence of forbidden bands at composition (x) calculated by the two approaches LDA and GGA for alloys $Al_xSc_{1-x}As$

5.2. Density of States

The electronic state density (DOS) for the $Al_xSc_{1-x}As$ alloys ($x = 0.00, 0.25, 0.50, 0.75,$ and 1.00) in phases B1 and B3 give an excess overview of the different states of the conduction and valence bands. The calculation of the total state density (TDOS) and of the partial state density (PDOS) for the alloys $Al_xSc_{1-x}As$, represented in (Fig.9), may be useful for identifying the character of the band states for a given composition x . The (Fig.9) shows that the region from the Fermi level to (-6.5 eV) is dominated by the states (As-4p, Sc-3d) in phase B1 for ScAs and the states (As-4p, Al-3s) in phase ZB (B3) for the binary compounds AlAs in approximation LDA and GGA. The TDOS and PDOS for the structure ZB (B3) of the alloy $Al_{0.50}Sc_{0.50}As$, in (Fig.10), show that the conduction band is dominated by the Sc-3d and Al-3s

states in this ternary alloy. As the composition of *Al* increased, the Scandium peak moved towards the Fermi level, as shown clearly in (Fig.10). The lower region of the valence band is completely occupied by As-4p and Al-3s states.

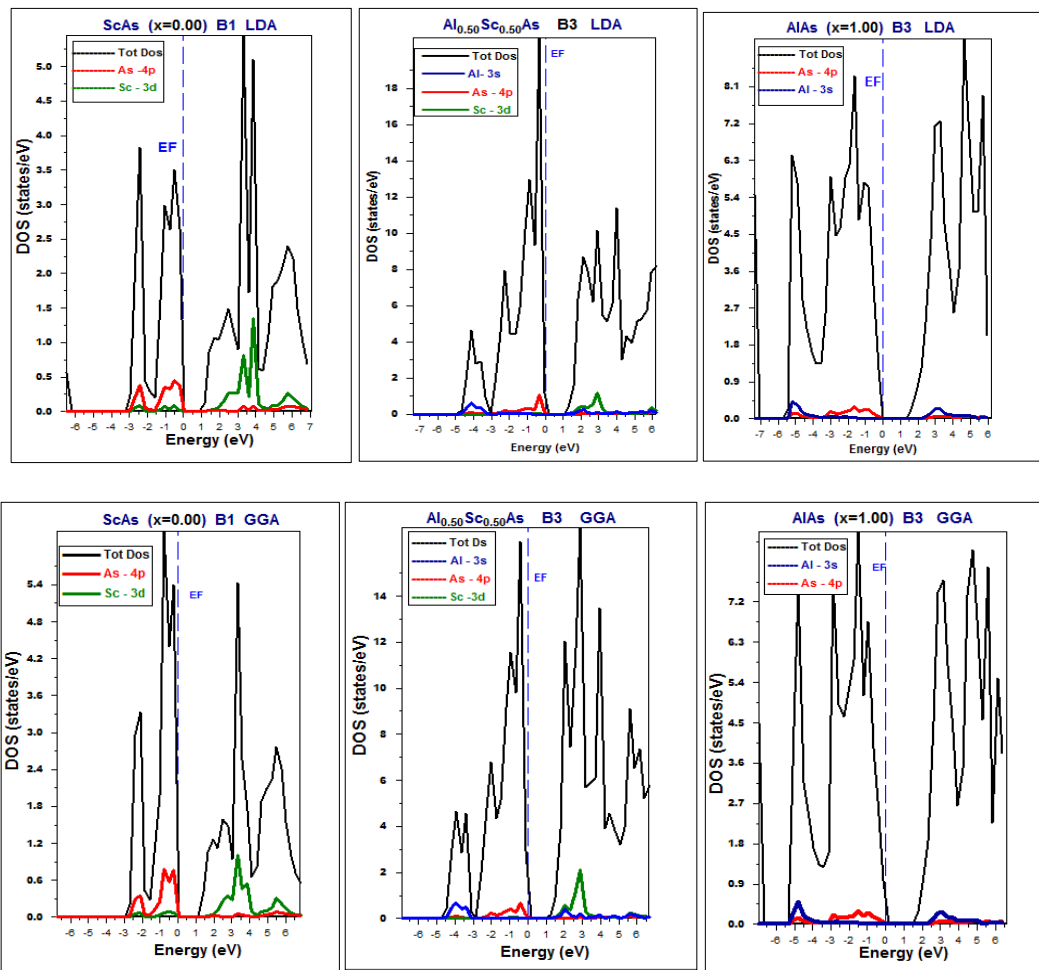


Figure 9. Presentation of the total state density and partial state density of the alloy $Al_xSc_{1-x}As$ $x = 0.00$ in phase RS (B1) and $x = 0.50$ and 1.00 in phase ZB (B3) by LDA and GGA

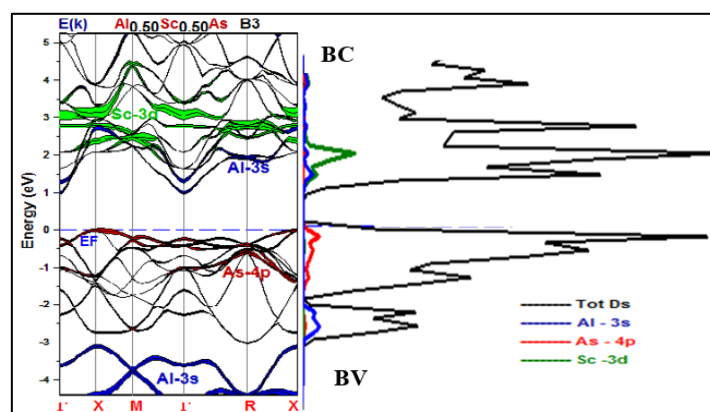


Figure 10. Graphical presentation of the total state density (TDOS) and partial state density (PDOS) of the alloy $Al_{0.50}Sc_{1-0.50}As$, in phases RS (B1) and ZB (B3) by LDA and GGA

6. Thermal properties

In general, the thermal properties, especially the melting point T_m and the Debye temperature θ_D of solids correlate strongly with their elastic properties [22-24]. For materials with cubic structures, the melting point T_m is adjusted to the bulk modulus B as follows: $T_m = 9.3 B + 607$, where T_m is given in Kelvin, while B is given in GPa [23]. Using this formula, the melting point T_m of RS (B1) ScAs, ZB (B3) Al_{0.5}Sc_{0.5}As, and ZB (B3) AlAs were found to be equal to 1406, 1192.5 and 1198 K, respectively. Unfortunately, to the best of the authors' knowledge, the melting point T_m of RS (B1) ScAs compound and ZB (B3) Al_{0.5}Sc_{0.5}As alloy have never been previously reported in the literature to make comparison.

7. Optical Properties

Optical properties are characterized by the dielectric function, the absorption coefficient, the electronic energy loss function and the refractive index as a function of photon energy, which is strongly linked to wavelength. In addition, optical properties, like all properties, are influenced by pressure and temperature.

The dielectric function $\varepsilon(\omega)$ describes the behavior of the material when excited by a light beam and comprises two parts, the imaginary part $\varepsilon_{Im}(\omega)$ and the real part $\varepsilon_{Re}(\omega)$ which is the derivative of the imaginary part. The formula for the total dielectric function according to *A. Gueddim et al, O. Stenzel et al* [20, 25] is given by :

$$\varepsilon(\omega) = \varepsilon_{Re}(\omega) + i\varepsilon_{Im}(\omega) \quad (8)$$

Where the real part is written as:

$$\varepsilon_{Re}(\omega) = \frac{1}{\pi} \wp \int_{-\infty}^{\infty} \frac{\varepsilon_{Im}(\omega')}{\omega' - \omega} d\omega' \quad (9)$$

$$\varepsilon_{Im}(\omega) = -\frac{1}{\pi} \wp \int_{-\infty}^{\infty} \frac{\varepsilon_{Re}(\omega')}{\omega' - \omega} d\omega' \quad (10)$$

Where \wp is the principal value.

The optical properties will be processed by LDA and GGA at $x=0$ in the RS (B1) phase and $x=0.25, 0.50, 0.75$ and 1 in the ZB (B3) phase.

The electron energy loss function $L(\omega)$

This function interprets the electron-matter interaction and the inelastic scattering of electrons in a material as a function of light excitation or temperature. These parameters are essential for understanding spectroscopy (study of the interaction between the material and

electromagnetic radiation) and photoelectric (electrons ejected from the cross-section of the material when excited by light). However, the optical constants of most compounds are unknown in the energy range from 10 to 50 eV, where electron-solid interactions are strong. Calculations are made in the energy range 0 to 13.6 eV. The real part $\epsilon_{Re}(\omega)$ on the (Fig.11) of the optical spectrum of the $Al_xSc_{1-x}As$ alloy at zero pressure as a function of photon energy is strongly related to wavelength. Its maximum is reached for a photon energy of about 1.63, 2.18, 2.72 and 3.26 eV for concentrations $x=0, 0.25, 0.50, 0.75$ and 1. It also reaches a minimum below zero for a photon energy of about 4.35, 3.81, 3.26, 3.81 and 4.89. The value at $x=1$ was compared with that found by S. Rameshkumar et al [26], with average relative errors of 0.02% was found. The maximum of the imaginary part $\epsilon_{Im}(\omega)$ in fig.8, is at 4.08, 3.26, 2.99, 3.54 and 4.08 eV respectively for concentrations $x=0, 0.25, 0.50, 0.75$ and 1 these points represent a limit beyond which an optical transition begins as a function of the gap energy. Consequently, the dielectric function is strongly dependent on the transition that occurs within the energy bands.

On the other hand, the spectrum of the energy loss function $L(\omega)$ is presented in Fig.12. We observe the significant peaks at 8.44, 6.53, 3.81, 4.89 and 9.52 eV. Comparing the value at $x=1$ with that found by S. Rameshkumar et al [26] and H. Shinotsuka et al [27] obtained experimentally, with a difference of 0.002% was found. It is for this reason that this rich material will give rise to so many studies in future research.

The refractive index n of a material is one of the most important optical parameters. Its study is a prerequisite for very distinct applications in optoelectronic structures such as optical fibers and photovoltaic cells. According to *T. Peng et al* [28] the refractive index calculated by the following equation:

$$n(\omega) = \sqrt{\frac{\epsilon_1(\omega) + \sqrt{(\epsilon_1^2(\omega) + \epsilon_2^2(\omega))}}{2}} \quad (11)$$

In the case where $(\omega=0)$, these are low frequencies, equation (8) will be:

$$n(0) = \sqrt{\epsilon_1(0)} \quad (12)$$

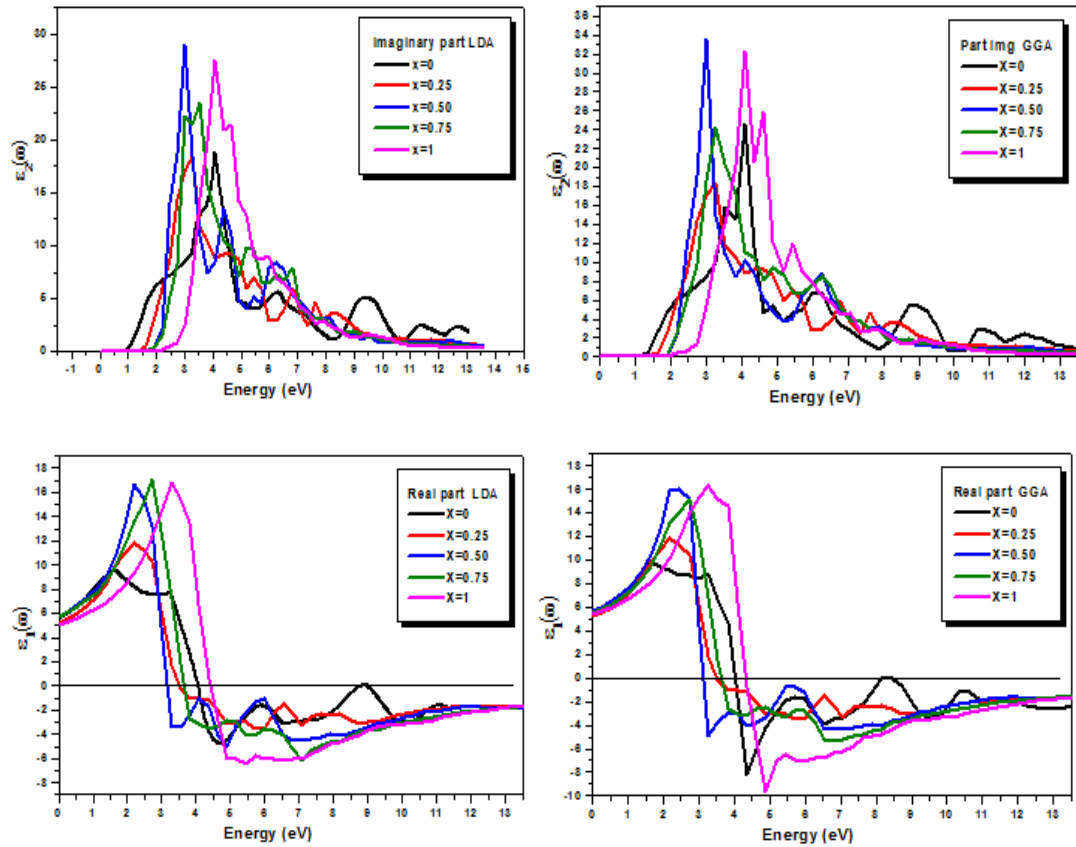


Figure 11. Graphical representation of the imaginary and real dielectric functions and the energy loss of the $\text{Al}_x\text{Sc}_{1-x}\text{As}$ alloy as a function of energy calculated by LDA and GGA

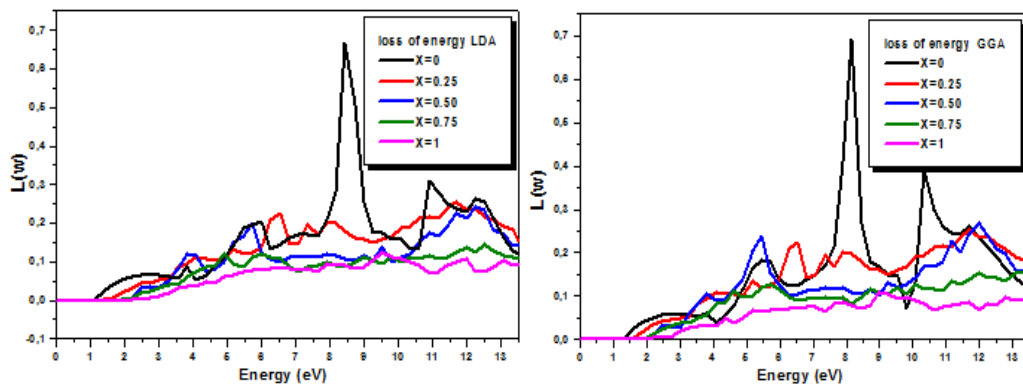


Figure 12. Graphical representation of the energy loss function of the $\text{Al}_x\text{Sc}_{1-x}\text{As}$ alloy as a function of the energy calculated by LDA and GGA

Table 5 shows the values of the refractive indices, the real dielectric function and the gap energy of the $\text{Al}_x\text{Sc}_{1-x}\text{As}$ compound at Aluminium concentrations $x=0, 0.25, 0.50, 0.75$ and 1 . It can be seen that the LDA approximation underestimates the energy of the band gap of 0.038 eV, so it can be said that the optical parameters should be lower than the experimental values.

Table 5. Variation of refractive index values of crystalline material in the B3 phase

	$n(0)$			$\epsilon_1(0)$		$E_g(\text{eV})$		
	LDA	GGA	Other result	LDA	GGA	LDA	GGA	other result
ScAs	2.356	2.309	4.83 [29].	5.554	5.334	1.478	1.625	1.38 [31]
Al _{0.25} Sc _{0.75} As	2.289	2.249		5.243	5.058	1.048	1.108	
Al _{0.50} Sc _{0.50} As	2.403	2.374		5.776	5.634	1.383	1.421	
Al _{0.75} Sc _{0.25} As	2.396	2.345		5.742	5.499	1.53	1.622	
AlAs	2.396	2.312	2.93 [30]	5.049	5.345	1.400	1.542	1.53 [1]

Suplimentary point

During our study of the optical properties of our Al_xSc_{1-x}As alloy, we took into account that the refractive index depends strongly on the imaginary part (absorbance of light by the material) and the real part (transparency of the material). Therefore, according to our calculations of the optical properties, we were able to find the critical point of an optical transition from transparency to absorbance of the material in a very small photon energy range of 2.72 to 3.81 eV. It was also found that the energy loss of the material during excitation is minimal at concentrations $x=0, 0.25, 0.50, 0.75,$ and 1 respectively. Table 4 illustrates the transition points where the imaginary part will be greater than the real part and this indicates that the Al_xSc_{1-x}As semiconductor material will be a good light absorber.

Table 6. Evaluation of the critical points of the optic transition of the alloy Al_xSc_{1-x}As at $x=.0, 0.25, 0.50, 0.75$ et 1

Concentration x	E(eV) photon	$\epsilon_{Img}(\omega)$	$\epsilon_{Rel}(\omega)$	$L(\omega)$
ScAs	2.99	8.43	7.35	0.067
Al _{0.25} Sc _{0.75} As	2.72	14.32	10.38	0.042
Al _{0.50} Sc _{0.50} As	2.99	28.96	4.92	0.036
Al _{0.75} Sc _{0.25} As	2.99	22.26	12.82	0.034
AlAs	3.81	19.89	13.53	0.034

8. Conclusions

Results predict that Al_xSc_{1-x}As alloys are good candidates for use in the design and production of electronic and optoelectronic devices in the future. In the absence of experimental studies on Al_xSc_{1-x}As alloys, we hope that this study will inspire future experimental research on these alloys. According to the simulation which there is effected, they conclude that by making vary complete energy, it was possible to note that B3 phase turns out to be more stable than B1 phase on surrounding conditions, for the alloy Al_xSc_{1-x}As in ($x = 0.25, x = 0.50, x = 0.75$ and 1.00) while for $x = 0.00,$ B1 is more stable using both LDA and GGA.

Concerning the lattice constants for the structure B3, according to *Vegard's law* with a slight deviation from a linear dependence in composition x . The difference is more pronounced in the structure B1. Moreover, it has been seen that the phase transition occurs around $x < 0.25$. In the case of $\text{Al}_x\text{Sc}_{1-x}\text{As}$, the transition $\text{B3} \rightarrow \text{B1}$ occurs at $x = 0.15$ per LDA. Thus, it can be concluded that below this value, it is preferable to manufacture a system of $\text{AlAs}/\text{Al}_x\text{Sc}_{1-x}\text{As}$ material because AlAs and $\text{Al}_x\text{Sc}_{1-x}\text{As}$ both crystallize in the structure B3. However, for $x > 0.15$, it is preferable to manufacture a $\text{ScAs}/\text{Al}_x\text{Sc}_{1-x}\text{As}$ material system because the two materials should crystallize in the structure B1 with a grating offset of only 0.037% for the $\text{ScAs}/\text{Al}_{0.50}\text{Sc}_{0.50}\text{As}$ system. As a result, a linear variation is observed and it can be reported that our alloy $\text{Al}_x\text{Sc}_{1-x}\text{As}$ crystallizes in the structure B1 for composition x below 0.15 and 0.25, per LDA and per GGA. In addition, the same alloy $\text{Al}_x\text{Sc}_{1-x}\text{As}$ crystallizes in the B3 structure for composition x greater than 0.15 and 0.25, per LDA and per GGA. Because convergence tests have shown that, the compound ScAs and the associated ternaries $\text{Al}_x\text{Sc}_{1-x}\text{As}$ converge rapidly.

The calculated electronic properties show that the alloys $\text{Al}_x\text{Sc}_{1-x}\text{As}$ have a direct forbidden band (Γ - Γ) for the composition $x = 0.25, 0.75, 1.00$ in the B3 structure and a direct forbidden band (X - X) for $x = 0.00$ in the B1 structure. Except for the composition $x = 0.50$, the alloy exhibits an indirect forbidden band (Γ - X) in phase B3, suggesting the possibility of their use in high-wavelength optoelectronic applications. Indeed, it will be noted that the B3 structure of the alloys $\text{Al}_x\text{Sc}_{1-x}\text{As}$ confirms mechanical stability under ambient conditions.

The melting point T_m of compound (B1) ScAs and alloy (B3) $\text{Al}_{0.5}\text{Sc}_{0.5}\text{As}$ has never before been reported in the literature for comparison.

We were able to determine the points of optical transition of the alloy at $x = 0, 0.25, 0.50, 0.75$ and 1, making it a good distinctive absorber for photovoltaic applications.

References

- [1] A. Srivastava, N. Tyagi, *High pressure behavior of AlAs nanocrystals: the first-principle study*, High Pressure Research: An International Journal 32, (2012) 43-47.
- [2] V. Nayak, U. P. Verma, *Study of Structural and Electronic Properties of ScN and ScAs in Rocksalt and Zincblende Structure* 1675, American Institute of physics. (2015).
- [3] A. Tebboune, D. Rached, A. Benzair, N. Sekkal, A. H. Belbachir, *Structural and electronic properties of ScSb, ScAs, ScP and ScN*, Physica Status Solidi B, 243, (2006) 2788–2795.

- [4] Y. Junhui, G. Mao, K-H.Xue, J. Wang, *A new family of two-dimensional ferroelectric semiconductors with negative Poisson's ratio*, *Nanoscale* 12 (2020) 1-30.
- [5] W. Lopez-perez, N. Simon, R. Gonzalez, J. A. Rodriguez, *First-principles study of the structural, electronic, and thermodynamic properties of $Sc_{1-x}Al_xAs$ alloys*, *Phys. Status Solidi B*250, (2013) 2163–2173.
- [6] W. Kohn, L.J. Sham, *Self-Consistent Equations Including Exchange and Correlation Effects*, *Physical. Review.* 140 A (1965) 1133.
- [7] S.Y. Savrasov, Z. Kristallogr, *Program LMTART for Electronic Structure Calculations*, Newark, 220 NJ 07102, 555 (2005).
- [8] H. Rekab-Djabri, S. Louhibi-Fasla, *Structural and electronic properties of $Cu_xAg_{1-x}Cl$: First-principles study*, *Eur. Phys. J. Plus* 132 (2017) 471.
- [9] J.P. Perdew, Y. Wang, *Accurate and simple analytic representation of the electron-gas energy*, *Physical. Review. B* 45, (1992) 13244.
- [10] G. Gruner, *Density Waves in Solids*, Addison-Wesley Publishing Company 98, (2018).
- [11] Peierls R.E., *Quantum Theory of Solids*, Oxford University press 238, (1996).
- [12] Fröhlich. H, *On the theory of dielectric breakdown in solids*, *Proceedings of the. Royal. Society. Lon. Ser-A* 223 (1954).
- [13] A. Zunger, M.L. Cohen, *Electronic structure of $CuCl$* , *Physical. Review. B: Condens. Matter* 20 (1979) 1189.
- [14] F.D. Murnaghan, *The Compressibility of Media under Extreme Pressures*, *Proc. Natl. Acad. Sci. U.S.A.* 30, (1944) 244-247.
- [15] W. M. Yim, E. J. Stofko, and R. T. Smith, *Vapor Growth and Properties of $ScAs$ and ScP* . *Applied Physics* 43, (1972) 254-256.
- [16] S. Adachi, *Properties of Semiconductor Alloys: Group-IV, III–V and II–VI semiconductors*. Wiley Series in Materials for Electronic 282 (2009).
- [17] A. Maachou, B. Amrani, and M. Driz, *Theoretical investigation of the lowest electronic states of $ScSe$ molecule*, *Physica B*388, (2007) 384-389.
- [18] R. Ahmed, S. J. Hashemifar, H. Akbarzadeh, M. Ahmed, and F. E-Aleem, *Ab initio of structural and electronic properties of III-arsenid binary compounds*, *Comput. Mater. Sci.*39, (2007) 580-586.
- [19] S.T. Oyama, *The chemistry of transition metal carbides and nitrides*, Springer, Dordrecht 414 (1996) 28-52.
- [20] A. Gueddim, S. Zerroug, N. Bouarissa, *Band structure and optical prperties of plyinganiline polymer material*, *Journal of Luminescence.* 135 (2013) 243-247.

- [21] I. Vurgaftman, J. R. Meyer, and L. R. Ram-Mohan, *Band parameters for III-V compound semiconductors and their alloy*, J. Appl. Phys. 89 (2001) 5815-5875.
- [22] N. Bioud, X-W. Sun, S. Daoud, T. Song, R. Khenata, S. Bin Omran, *High-temperature and high-pressure physical properties of Cul with zinc-blende phase by a systematic ab initio investigation*, Optik, 155 (218) 17-25.
- [23] T. Özer, *Study of first principles on anisotropy and elastic constants of YAl₃ compound*, Canadian Journal of Physics 98 (2020) 357-363.
- [24] S. Daoud, N. Bioud, L. Belagraa, N. Lebga, *Elastic, Optoelectronic and Thermal Properties of Boron Phosphide*, J. Nano- Electron. Physics 14 (2013) 504061.
- [25] O. Stenzel, *The Physics of Thin Film Optical Spectra*, Springer Cham 44 (2016)2435.
- [26] S. Rameshkumar, G. Jaiganesh, V. Jayalakshmi, *Refractive index of AlAs and AlSb compounds: An ab-initio study*, Indian Journal of Science 14 (2015) 29-34.
- [27] H. Shinotsuka, H. Yoshikawa, S. Tanuma, *First Principles Calculations of Optical Energy Loss Function for 30 Compound and 5 Elemental Semiconductors*, Journal of Surface Science and Nanotechnology 19, (2021)70-87.
- [28] T. Peng, J. Piprek, *Refractive index of AlGaInN alloys*, Electronics Letters 32, (1996) 2285-2286.
- [29] S. K. Tripathy, *Refractive Indices of Semiconductors from Energy gaps*, Optical Materials 46 (2015) 240-246.
- [30] L. Boudaoud, W. Adli, R. Mechref, N. Sekkal, *Electronic properties of cubic ScGaAs and ScGaN ternaries and superlattices*, Superlattices and Microstructures 47, (2010) 361-368.